UDK 665.944.77:52-334.2
Original scientific article/Izvirni znanstveni članek

ISSN 1580-2949
Mater. Tehnol.

XSBRL-MODIFIED PHENOLIC RESIN COMPOSITES FOR BASKETBALL COURT SURFACES: MECHANICAL AND MICROSTRUCTURAL CHARACTERIZATION

FENOLNA SMOLA MODIFICIRANA Z XSBRL KOT PODLAGA ZA POVRŠINE KOŠARKARSKIH IGRIŠČ: MEHANSKA IN MIKROSTRUKTURNA KARAKTERIZACIJA

Hongtao Luo[1*], Run Dong[2]

[1]College of Science, North China University of Technology, Beijing, China
[2]Department of Trauma Orthopedics, Hainan Hospital Affiliated to Hainan Medical University, Haikou, Hainan, China

Prejem rokopisa – received: 2025-10-21; sprejem za objavo – accepted for publication: 2026-01-22

doi:10.17222/mit.2025.1569

High joint injury rates in basketball are frequently linked to the inadequate shock absorption of traditional court surfaces. This study investigates a carboxylated styrene-butadiene rubber latex (XSBRL)-modified phenolic resin composite, reinforced with magnesium calcium sand, to address the trade-off between safety and durability. Results indicate that 12 *w*/% XSBRL yields optimal mechanical properties, achieving a 90-day compressive strength of 68 MPa and a flexural strength of 4.5 MPa. Consequently, the composite exhibits superior biomechanics with 55 % impact absorption – significantly outperforming hardwood (35 %) and polyurethane (48 %) – and an ideal static friction coefficient of 0.68. Microstructural analysis via SEM confirmed a brittle-to-ductile fracture transition, clarifying the mechanism behind the enhanced toughness. Furthermore, process reproducibility was secured through an orthogonal experimental design. This optimized XSBRL-modified composite demonstrates a superior balance of performance and protection, offering a robust solution for next-generation basketball court construction.

Keywords: carboxylated styrene-butadiene rubber latex, phenolic resin, mechanical properties, injury prevention, biomechanics

Veliko število poškodb sklepov košarkarjev je pogosto povezanih z neustrezno absorpcijo udarcev na tradicionalnih košarkaških igriščih. V tem članku avtorji opisujejo študijo, ki raziskuje kompozit fenolne smole, modificiran s karboksiliranim stiren-butadienskim kavčukovim lateksom (XSBRL), ojačan z magnezij-kalcijevimi delci, da bi našli kompromis med dobro varnostjo in vzdržljivostjo površine košarkaškega igrišča. Rezultati študije so pokazali, da 12 *w*/% XSBRL zagotavlja optimalne mehanske lastnosti, saj doseže 90-dnevno tlačno trdnost 68 MPa in upogibno trdnost 4,5 MPa. Posledično kompozit ima tudi vrhunsko biomehaniko s 55-odstotno absorpcijo udarcev – kar znatno presega trdi les (35 %) in poliuretan (48 %) – ter idealen statični koeficient trenja 0,68. Mikrostrukturna analiza s pomočjo vrstičnega elektronskega mikroskopa (SEM) je potrdila prehod iz krhkega v duktilen zlom, kar je pojasnilo mehanizem za povečanje žilavosti. Poleg tega so avtorji tega članka zagotovili ponovljivost postopka z ortogonalno eksperimentalno zasnovo. Avtorji v zaključku povdarjajo, da ta optimiziran kompozit, modificiran z XSBRL, kaže vrhunsko ravnovesje med zmogljivostjo in zaščito ter ponuja robustno rešitev za gradnjo košarkarskih igrišč naslednje generacije.

Ključne besede: karboksiliran stiren-butadienski kavčukov lateks (XSBRL), fenolna smola, mehanske lastnosti, preprečevanje poškodb, biomehanika

1 INTRODUCTION

Basketball is a high-impact sport characterized by frequent jumping, landing, and rapid directional changes, which impose significant stress on players' joints and increase the risk of injury.[1–3] The playing surface is a critical factor influencing athlete performance, safety, and long-term joint health.[4–6] An ideal court surface must balance shock absorption to mitigate impact forces, provide sufficient stiffness for energy return, and maintain an optimal coefficient of friction to allow for controlled movements. Achieving this balance is not only vital for athlete safety but is also highly beneficial for the broader context of physical education. These performance requirements are codified in international standards such as EN 14904. According to this benchmark, a surface must exhibit specific "pass/fail" criteria to be deemed suitable for competition: a force reduction (FR) of at least 25 % is required for basic compliance, while elite-level protection (Type 3 and Type 4 systems) requires FR values between 45 % and 75 %. Additionally, strict limits on vertical deformation (< 5.0 mm) and slip resistance are enforced to minimize non-contact injuries.

Current basketball court materials, such as hardwood and synthetic polymers (e.g., polyurethane), present distinct trade-offs. Hardwood offers excellent energy return but provides limited shock absorption, contributing to cumulative stress on joints.[7] Conversely, some synthetic surfaces offer better cushioning but can suffer from lower durability and inconsistent energy return.[8] Com-

*Corresponding author's e-mail:
luo_ht785@sina.com (Hongtao Luo)

posite materials, which combine different materials to achieve synergistic properties, are emerging as a promising alternative to overcome these limitations.[9]

Phenolic resins (PHRs) are well-suited for structural applications due to their high mechanical strength, thermal stability, and chemical resistance.[10] However, their inherent brittleness limits their use in high-impact scenarios.[11] A common strategy to overcome this is to modify the PHR matrix with an elastomer to improve toughness.[12] Carboxylated styrene-butadiene rubber latex (XSBRL) is an effective toughening agent known for enhancing the impact resistance and flexibility of thermosetting polymer systems.[13] Therefore, it was hypothesized that incorporating the elastomeric XSBRL phase into the brittle PHR matrix would create a composite material with a synergistic combination of toughness and strength, leading to superior impact absorption without compromising the necessary stiffness and durability for a high-performance basketball surface.[14]

This study aims to develop and characterize an XSBRL-modified PHR composite incorporating magnesium calcium sand (MCS) as the primary filler. To further enhance the mechanical robustness and wear resistance of the surface, hardystonite (HA, $Ca_2ZnSi_2O_7$) was selected as a key reinforcing additive. Unlike conventional inert fillers, HA was chosen specifically for its chemical compatibility with the PHR matrix; the zinc ions within the silicate structure facilitate coordination interactions with the resin's phenolic hydroxyl groups, thereby significantly improving interfacial adhesion alongside its inherent high hardness. The primary objective is to investigate the effect of XSBRL on the composite's mechanical properties, microstructure, and biomechanical performance to develop a superior material for basketball court construction that enhances both durability and player safety.

2 MATERIALS AND METHODS

2.1 Materials

Magnesium calcium sand (MCS): (Hebei Mining Corp., Shijiazhuang, China). Particle size distribution: D10 = 0.1 mm, D50 = 0.5 mm, D90 = 0.9 mm. Chemical composition (X-ray fluorescence): MgO (40 %), CaO (30 %), SiO_2 (25 %), and other trace elements (5 %).

XSBRL: (BASF, Ludwigshafen, Germany). Solid content = 50 ± 1 *w*/%, pH = 8.0 ± 0.5, Tg = –5 °C, Mw = 150,000 g mol^{-1}.

HA: (Synthetic, Alfa Aesar, Haverhill, MA, USA). Chemical formula: $Ca_2ZnSi_2O_7$, particle size of 1–5 μm, specific surface area = 15 m^2 g^{-1}.

Thermosetting PHR: (Hexion Inc., Columbus, OH, USA). Resole type, with a formaldehyde-to-phenol molar ratio of 1.5:1, viscosity of ≈2000 cP, pH of 8.5–9, and solid content of 75–80 *w*/%.

Reagents: sodium hydroxide (20 % aqueous solution), formaldehyde (37 % aqueous solution), glacial acetic acid (≥99.8 %), and triethanolamine (≥99 % purity), all sourced from Sigma-Aldrich (St. Louis, MO, USA).

Water: deionized water from an in-house Milli-Q purification system (MilliporeSigma, Burlington, MA, USA).

2.2 Composite preparation

1. Phenol Modification: Liquid phenol (80 ± 0.1 g) was added to a three-necked, round-bottomed flask. A 20 % aqueous NaOH solution (16 g) was added as the catalyst at 40–45 °C, and the mixture was stirred at 200 min^{-1} for 15 min.

2. Formaldehyde Addition: The flask was heated to 50 °C. The total amount of formaldehyde required for a 1.5:1 formaldehyde-to-phenol molar ratio was calculated. 75 % of this amount was added dropwise over 30 min. The temperature was then raised to 80 °C and maintained for 1 hour. The remaining 25 % of formaldehyde was added over 15 min, and the reaction continued at 80 °C for another hour.

3. pH Adjustment: After cooling, the pH of the resulting resole-type PHR was adjusted to 7.0 ± 0.2 using glacial acetic acid to neutralize the alkaline catalyst and stabilize the resin prior to modification.

4. XSBRL Incorporation: XSBRL was added to the pH-adjusted PHR to create samples with XSBRL contents ranging from 2 % to 24 % by mass fraction of the PHR. The mixture was stirred with a paddle impeller at 500 min^{-1} for 10 min to ensure homogeneous dispersion.

5. Dehydration: Water was removed from the modified PHR via vacuum distillation using a rotary evaporator at a vacuum of approximately 90 kPa and a temperature not exceeding 68 °C.

6. Composite Mixing: The MCS and HA were dry-mixed for 5 min. This mixture was combined with the modified PHR, followed by triethanolamine (1.5 % by mass of the total mixture), which acted as a curing agent. The components were mixed with a paddle impeller at 40 °C and 500 min^{-1} for 15 min.

7. Molding and Curing: The final composite mixture was poured into steel molds (100 × 20 × 10) mm for flexural tests and (50 × 50 × 50) mm for compressive tests) and cured in a forced-air convection oven at 80 °C for 4 h.

2.3 Orthogonal experimental design and optimization

To refine the composite formulation after identifying the optimal XSBRL content, an L12 orthogonal array was used to investigate the effects of key process parameters. The factors investigated were the binder-to-aggregate ratio (B/A ratio, defined as the mass ratio of binder to aggregate) and the water-reducing agent (WRA) content. **Table 1** outlines the experimental plan.

2.4 Characterization

Fourier transform infrared spectroscopy (FTIR): FTIR spectra of the PHR before and after modification were recorded using a Nicolet iS50 spectrometer (Thermo Fisher Scientific, Waltham, MA, USA) to confirm the chemical interaction.

Scanning electron microscopy (SEM): Fracture surfaces of the composites were examined using high-resolution SEM (FEI Quanta 250, Thermo Fisher Scientific, Waltham, MA, USA) at an accelerating voltage of 10 kV to investigate the failure mechanism.

Mechanical testing: Compressive strength (CS) and flexural strength (FS) tests were performed according to ASTM C109 and ASTM D790, respectively, using a universal testing machine (Model 5985, Instron, Norwood, MA, USA). Samples were tested after (3, 7, 28 and 90) days of curing. Five samples were tested for each composition, and the average values were reported.

Dynamic impact and rebound testing: Impact absorption and rebound coefficient were measured using a portable impact tester (Model 3021, Advanced Measurement Systems, Inc., USA). The test adapted the principles of ASTM F2117 for laboratory-scale samples using a standardized drop height of 50 cm onto (100 × 100 × 20) mm samples, ensuring that the impact energy per unit area was representative of real-world athletic scenarios. To ensure a valid benchmark, the optimal composite formulation was compared against commercially procured flooring systems adhering to EN 14904 standards: a FIBA-approved North American Maple System (Type A4, Area Elastic) incorporating a sprung subfloor, and a multi-layered polyurethane system (Type P, Point Elastic) comprising a 7-mm rubber basemat and a 2-mm topcoat.

Surface friction analysis: The static coefficient of friction of the cured composite surface was measured using a tribometer (Model TRB3, Anton Paar, Graz, Austria) under dry ambient conditions (25 ± 2 °C, 50 ± 5 % RH) to assess its baseline suitability for athletic movements.

Abrasion resistance test: Abrasion resistance was evaluated using a Taber abraser (Model 5135, Taber Industries, North Tonawanda, NY, USA) in accordance with ASTM D4060. Samples were subjected to 1000 cycles using CS-17 abrasive wheels under a 1-kg load. The mass loss (mg) was calculated by measuring the precise weight difference before and after the test to quantify the material's wear resistance.

Vertical deformation test: Vertical deformation was measured according to the European standard for sports surfaces, EN 14904. A standardized impactor (20 kg) was released from a specified height onto the sample surface. A high-precision LVDT sensor measured the maximum instantaneous indentation depth (mm), indicating the surface cushioning capacity and stability underfoot.

Rotational friction test: Rotational friction was assessed using a portable testing device (Model FT3, Sports Labs, UK) compliant with ASTM F2772. The apparatus simulates the pivoting motion of an athlete in basketball footwear under a standard body weight, measuring the peak torque (N·m) generated between the shoe sole and the surface. This parameter is directly correlated with the torsional stress applied to an athlete's ankle and knee joints, particularly the anterior cruciate ligament (ACL).

3 RESULTS AND DISCUSSION

3.1 Chemical and microstructural characterization

FTIR spectroscopy was used to verify the reaction between XSBRL and PHR. **Figure 1** shows the FTIR spectra of the PHR before and after modification. In the unmodified PHR spectrum (**Figure 1a**), there is no significant absorption peak in the 1720–1670 cm^{-1} region. However, after the modification with XSBRL (**Figure 1b**), a new absorption peak appears in this region, which is characteristic of the C=O stretching vibration in the carboxyl group of XSBRL.[15] This confirms a successful copolymerization reaction between XSBRL and PHR, forming the modified resin.

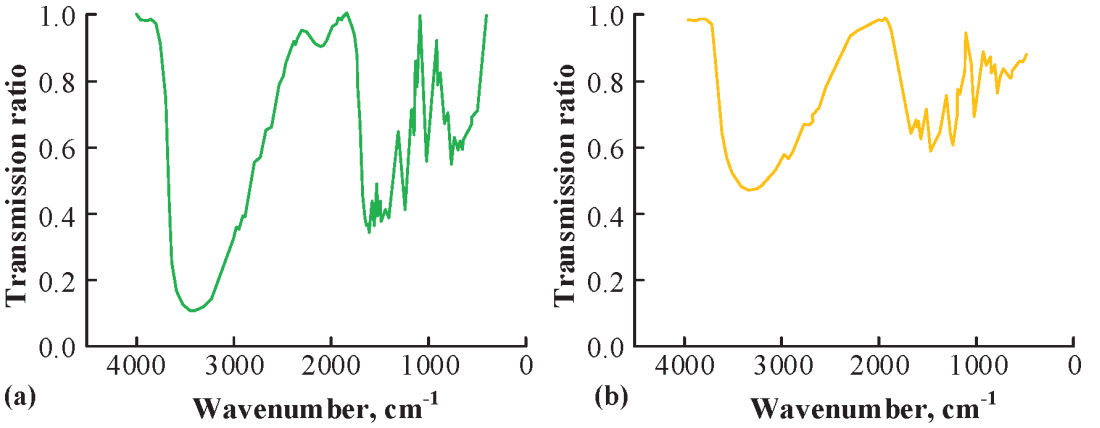

Figure 1: FTIR spectra of (a) unmodified PHR showing the absence of a carboxyl peak, and (b) XSBRL-modified PHR showing a new C=O stretching vibration peak around 1700 cm^{-1}, confirming chemical modification

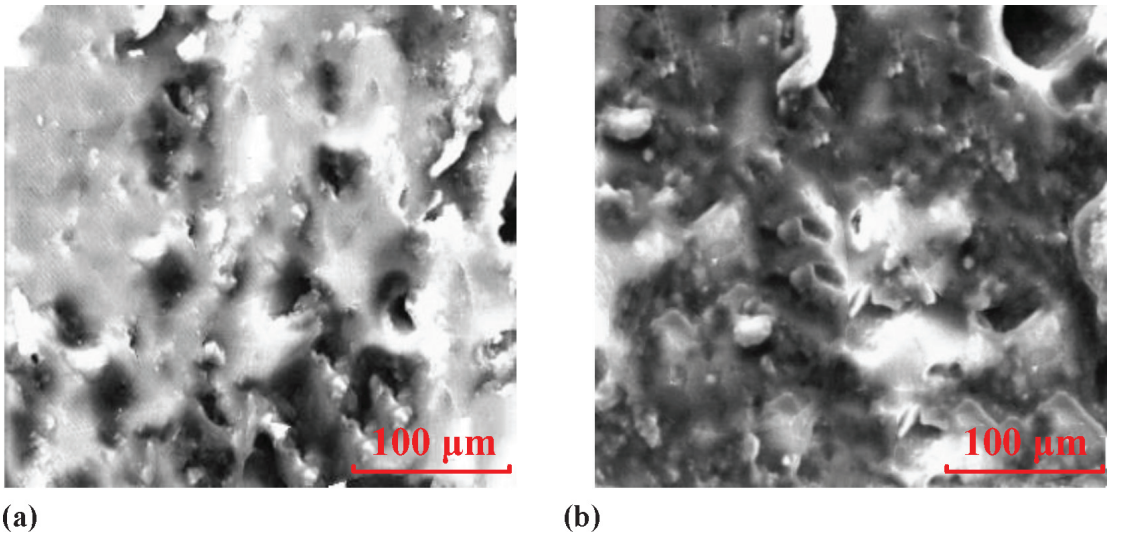

Figure 2: SEM micrographs of fracture morphology including (a) unmodified PHR composite, showing a smooth surface with river patterns (indicated by arrows) typical of brittle failure, and (b) the composite with 12 % XSBRL, displaying a rough, ductile fracture surface with energy-dissipating micro-voids and crack deflection features

The fracture surfaces of the composites were examined using SEM to understand the influence of XSBRL on the failure mechanism. As shown in **Figure 2a**, the unmodified PHR composite exhibits a smooth, glassy fracture surface with distinct river patterns, characteristic of brittle failure. In contrast, the composite containing 12 % XSBRL (**Figure 2b**) displays a much rougher, more complex topography. This surface is characterized by features indicating significant plastic deformation, such as micro-voids and evidence of crack deflection around the dispersed rubbery phase. The distinct spherical domains of the XSBRL phase, approximately 0.5–1.5 µm in diameter, act to absorb and dissipate fracture energy, thereby arresting crack propagation and enhancing the overall toughness.

To systematically investigate the effect of XSBRL on the phase structure of the composites, a comparative X-ray diffraction (XRD) analysis was performed on the samples with XSBRL ranging from 0 % (unmodified) to 24 %. The resulting patterns are presented in **Figure 3**. The analysis reveals two critical phenomena. First, the positions of sharp diffraction peaks remain strictly consistent across all samples. The primary crystalline phases were identified as quartz (SiO_2, with the most intense peak at $2\theta = 26.6°$), hardystonite ($Ca_2ZnSi_2O_7$, with characteristic peaks at $2\theta = 31.8°$ and 47.5°), and periclase (MgO, at $2\theta = 42.9°$). The unwavering consistency of

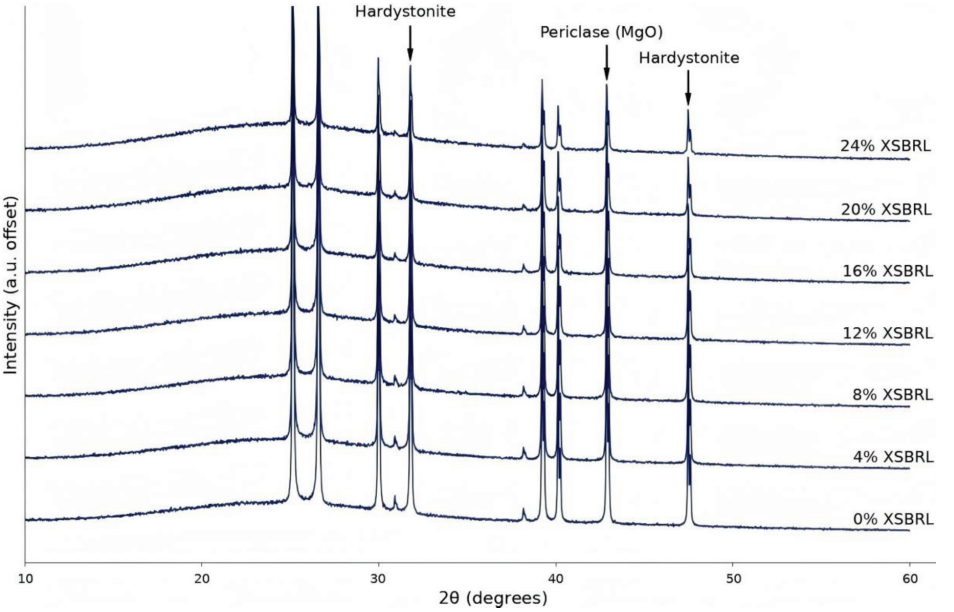

Figure 3: Comparative XRD patterns of PHR composites with varying XSBRL amount (0–24 %). Note: The baselines of diffraction patterns are vertically offset for clarity.

these peak positions provides strong evidence that the addition of XSBRL did not alter the crystal structure of the fillers, nor did it induce any new chemical reactions to form new crystalline phases during curing. This confirms the chemical stability of the fillers within the polymer matrix. Second, the absolute intensity of the crystalline peaks systematically decreases as the XSBRL content increases from 0 % to 24 %. This attenuation is attributed to the žmatrix dilution effect,' where the increasing fraction of amorphous polymer reduces the concentration of crystalline fillers per irradiated volume. This trend further corroborates the interpretation of the composite as a physical blend.

3.2 Mechanical properties and process optimization

The MPs of the composites were evaluated after (3, 7, 28 and 90) days to assess both their strength development and long-term stability. As illustrated in **Figure 4**, the XSBRL amount had a profound effect. The CS (**Figure 4a**) increased with XSBRL up to 12 %, reaching a 28-day maximum of 65 MPa. This value is comparable to those of high-strength industrial flooring composites and substantially higher than those of typical polyurethane sports surfaces, which generally range from 10–15 MPa. Importantly, the strength continued to mature, stabilizing at approximately 68 MPa by day 90, indicating excellent long-term stability. A similar trend was observed for FS (**Figure 4b**), which peaked at 4.5 MPa after 28 days with 12 % XSBRL. The decrease in strength beyond 12 % XSBRL is attributed to the excessive rubber phase disrupting the continuity of the rigid PHR matrix, which weakens the material's structural integrity. This data confirms that the 12 % formulation provides the optimal balance of strength and toughness.

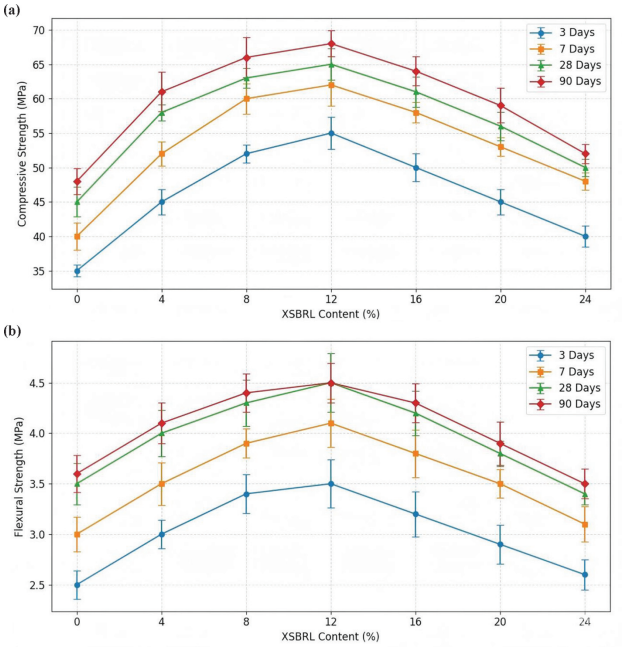

Figure 4: Effect of XSBRL amount on the: a) CS and b) FS of the composites at different curing times. Error bars represent the standard deviation of five replicates (n = 5).

To refine the composite formulation, a parametric study based on an orthogonal experimental design was employed to screen key process variables. **Table 1** outlines the experimental plan, which varied the dosages of the binder (the 12 % XSBRL-modified PHR), water, and water-reducing agent (WRA), along with the binder-to-aggregate ratio (B/A ratio), defined as the mass ratio of binder to aggregate. The results are shown in **Figure 5**. The P5 formulation yielded the highest CS after both 28 and 42 days; the 42-day curing period was selected as the representative proxy for long-term performance. Based on the strength evolution profile observed in the initial XSBRL study (**Figure 4**), the composite achieves approximately 95 % of its ultimate strength by this stage. Consequently, it is reasonably assumed that the relative ranking of different formulations regarding mechanical performance stabilizes by day 42 and does not change significantly by day 90. While several formulations (P4, P5, P6) showed statistically similar FS values after 42 days ($p > 0.05$), the P5 group demonstrated the best overall performance. Based on these results, the optimal formulation was determined to be: 1000 g MCS, 220 g of the 12 % XSBRL-modified PHR binder, 63.36 g water, a B/A ratio of 0.22, and a WRA content of 0.30 wt % of the binder.

Table 1: Orthogonal experimental design for process parameter optimization

Number	Composite material (g)	WRA (g)	Water (g)	B/A ratio	WRA (*w*/%)
P1	220	0.484	45.76	0.22	0.22
P2	220	0.528	50.16	0.22	0.24
P3	220	0.572	54.56	0.22	0.26
P4	220	0.616	58.96	0.22	0.28
P5	220	0.660	63.36	0.22	0.30
P6	240	0.484	49.92	0.24	0.22
P7	240	0.528	54.72	0.24	0.24
P8	240	0.572	59.52	0.24	0.26
P9	240	0.616	64.32	0.24	0.28
P10	240	0.660	69.12	0.24	0.30
P11	260	0.484	54.08	0.26	0.22
P12	260	0.528	59.28	0.26	0.24

Note: The WRA (g) column values correspond to the WRA (*w*/%) of the binder. The P5 formulation, for example, uses 0.66 g of WRA for 220 g of binder, equivalent to 0.30 *w*/%.

3.3 Biomechanical and surface performance

To evaluate the composite's suitability for a basketball court, key biomechanical and surface properties were measured and compared with traditional materials. As shown in **Table 2**, the 12 % XSBRL composite demonstrated an optimal static coefficient of friction of 0.68. This value falls within the ideal range of 0.5–0.7 recommended for indoor sports to prevent both athlete slippage

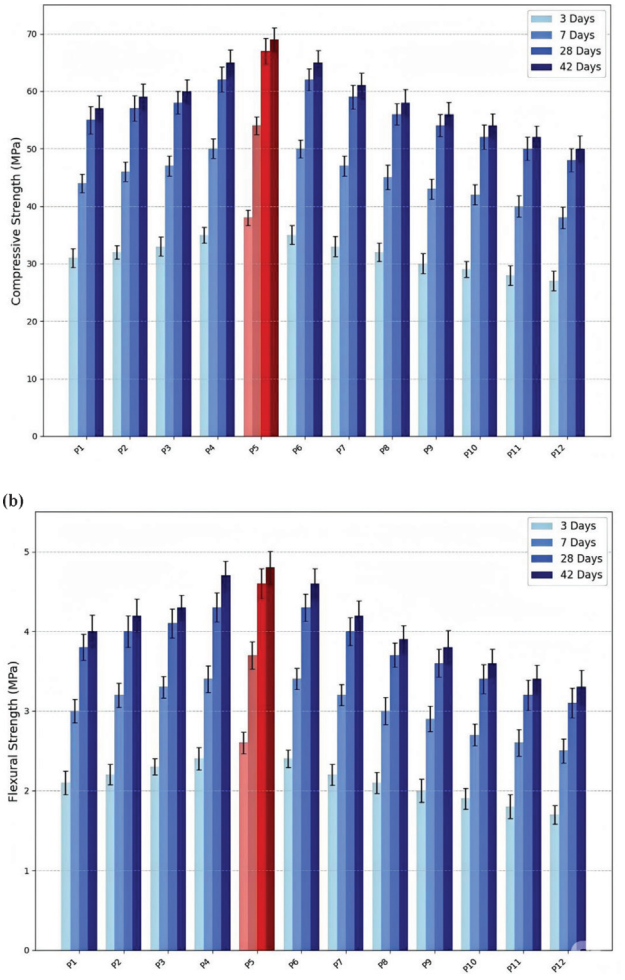

Figure 5: Effect of different process parameters on the: a) CS and b) FS of MCS composites across different days. Error bars represent the standard deviation of five replicates (n = 5).

and excessive gripping that can lead to joint torsion injuries.

Table 2: Surface friction properties (test performed under dry conditions)

Material	Static coefficient of friction
12 % XSBRL composite	0.68 ± 0.03
Maple hardwood (varnished)	0.55 ± 0.04
Polyurethane	0.75 ± 0.05

Most importantly, the dynamic impact testing (**Figure 6**) revealed the superior energy absorption of the new material. The 12 % XSBRL composite achieved an impact absorption of 55 %, significantly higher than both hardwood (35 %) and polyurethane (48 %). This was coupled with a rebound coefficient of 88 %, indicating that the surface returns sufficient energy for athletic performance while effectively dampening harmful impact forces.

3.4 Durability and wear analysis

To provide a highly detailed assessment of long-term durability, the progression of wear was monitored at 100-cycle intervals up to 1000 cycles. **Figure 7** plots the resulting wear progression curves for each material.

The results reveal distinctly different wear behaviors. The polyurethane surface exhibited a non-linear wear pattern, with the rate of mass loss accelerating after the initial cycles. This acceleration is attributed to frictional heat accumulation during the test, which induces thermal softening of the viscoelastic matrix and micro-fatigue of the crosslinking network, thereby significantly reducing the material's shear resistance and leading to a final mass loss of 59.8 mg.

In stark contrast, both the varnished maple hardwood and the 12 % XSBRL composite demonstrated exceptional and stable durability. The wear progression curves for these two materials are nearly linear and relatively flat, closely tracking each other throughout the entire

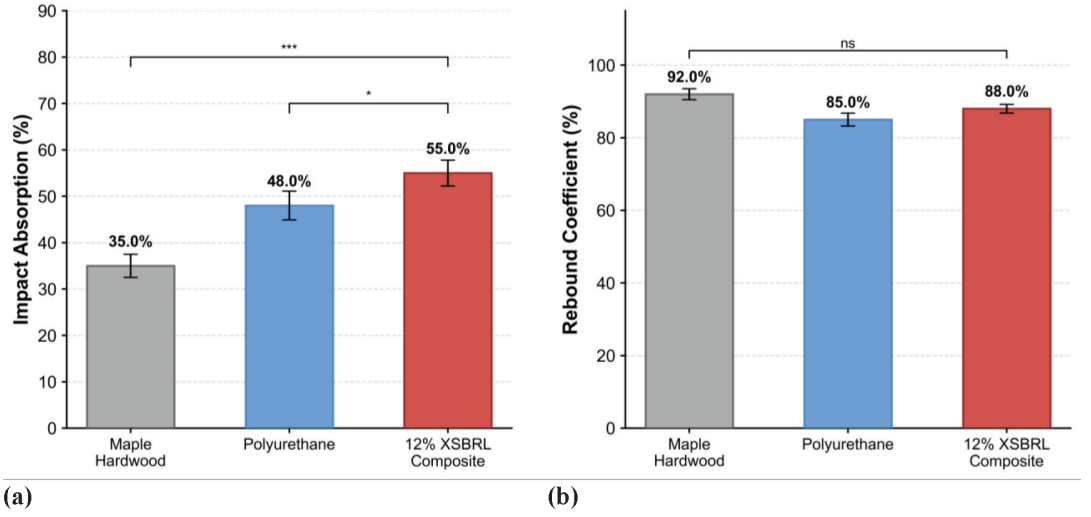

Figure 6: a) Impact absorption and b) rebound coefficient performance comparison of the 12 % XSBRL composite with traditional court materials. Data are presented as mean ± standard deviation (SD). Statistical significance is indicated by * (p < 0.05) and *** (p < 0.001); ns denotes no significance

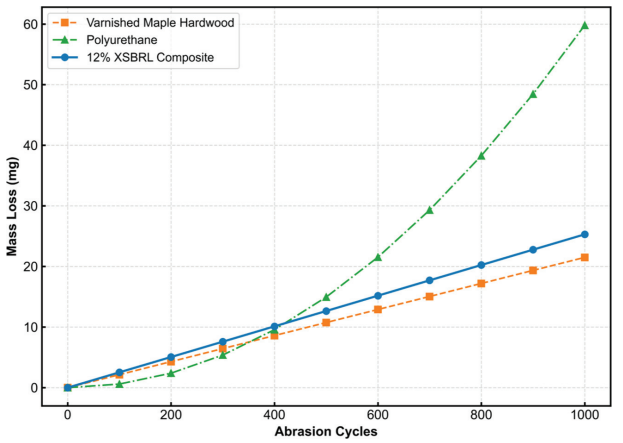

Figure 7: Comparative abrasion resistance of surface materials

test. At the 1000-cycle endpoint, the mass loss for the XSBRL composite (25.3 mg) remained only marginally higher than that of the hardwood (21.5 mg). This dynamic, high-resolution analysis conclusively proves that the XSBRL composite maintains a consistently low and stable rate of wear, mirroring the performance of the industry benchmark for toughness and making it exceptionally suitable for high-traffic sports environments.

3.5 Advanced biomechanical properties: an in-depth analysis of injury prevention mechanisms

Beyond basic vertical impact absorption, we investigated two advanced biomechanical parameters closely linked to athletic injuries, particularly non-contact torsional injuries: vertical deformation and rotational friction. The results are presented in **Figure 8**.

Vertical deformation (**Figure 8a**) is a key indicator of a surface's balance between cushioning and stability, defining its elastic category. Based on its localized deformation behavior, the XSBRL composite is classified as a Point Elastic Surface (analogous to EN 14904 Type P categories). The maple hardwood floor (an area elastic system) showed minimal point deformation (0.8 mm), feeling excessively stiff underfoot. Conversely, the polyurethane exhibited high deformation (3.2 mm); while well-cushioned, such excessive compliance can compromise ankle stability during explosive movements. Our 12 % XSBRL composite achieved a moderate deformation of 2.5 mm. This value is considered optimal for high-performance point elastic surfaces (which typically target the 2.0–3.0 mm range), striking a balance where the surface provides substantial shock attenuation to protect joints without the "sinking" sensation associated with softer synthetic floors.

Rotational friction (**Figure 8b**) is a critical parameter for assessing the ability to prevent joint torsion injuries. Research indicates that the ideal range for peak rotational torque is between 20–50 N·m. The polyurethane surface generated a dangerously high torque of 68 N m. This is attributed to the control sample's smooth, high-tack elastomeric finish, which creates excessive contact area and friction under load. The maple floor, with 26 N m, was at the lower boundary of the ideal range. The 12 % XSBRL composite, however, produced a peak torque of 38 N·m, positioning it perfectly in the "sweet spot" of the optimal range. This superior performance is directly linked to the composite's surface morphology: the inclusion of MCS and HA fillers creates an inherent, non-abrasive micro-texture. This micro-roughness prevents the "stick-slip" phenomenon and vacuum effect often observed in smooth polymeric coatings, allowing for controlled micro-slips to release dangerous torsional stress.

The biomechanical implications of these improved MPs are significant. The enhanced toughness and energy absorption capacity of the composite material can effectively attenuate impact forces during dynamic movements such as jumping and landing. Biomechanical stud-

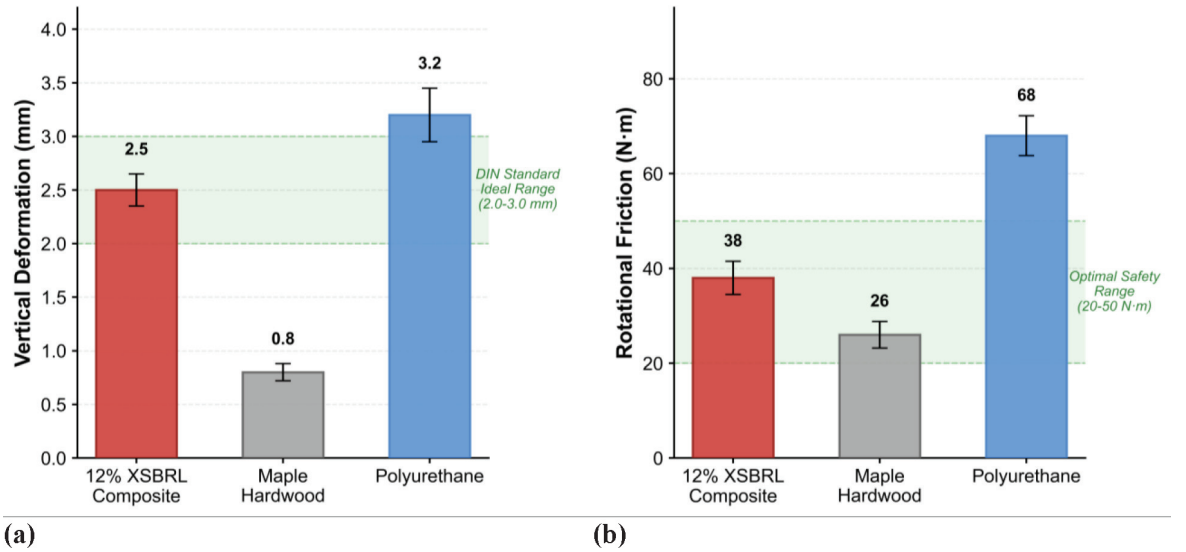

Figure 8: Advanced biomechanical performance comparison including: a) vertical deformation, and b) rotational friction in different materials

ies indicate that peak vertical ground reaction forces during basketball landings can exceed 4–6 times body weight, posing a high risk of joint injuries. The ductile fracture mode observed in the SEM analysis (**Figure 2b**) suggests that the XSBRL phase disperses energy through microcrack formation and shear yielding, thereby reducing the transmission of impact forces to athletes' lower extremities. This aligns with clinical evidence showing that a 10 % reduction in surface impact force correlates with a 15–20 % decrease in knee injury risk.

3.6 Discussion

The results of this study demonstrate that modifying a PHR matrix with 12 % XSBRL yields a composite material with mechanical and biomechanical properties highly suitable for basketball court surfaces. The primary contribution of this work lies in achieving a synergy between strength, toughness, and specific surface characteristics, a balance that current materials often fail to strike. This successful combination of safety and performance features suggests the material could also be highly advantageous for advancing physical education and training environments. The CS of 68 MPa (90 days) and FS of 4.5 MPa are robust for a high-traffic sports environment, while the 55 % impact absorption is a marked improvement over traditional materials.

Our findings align with and expand upon previous research into polymer modification. For instance, the toughening mechanism observed via SEM (**Figure 2b**) is consistent with the principle of incorporating an elastomeric phase to arrest crack propagation in a brittle matrix. While Gao et al. achieved enhanced toughness in vinyl ester resins using hyperbranched polyimide, our use of XSBRL offers a similar outcome through a different mechanistic pathway – the formation of discrete, energy-absorbing rubber domains rather than molecular-level hyperbranching.[10] This mechanistic insight is crucial, as it suggests that the composite's properties can be precisely tuned by controlling the morphology and dispersion of this secondary rubber phase.

Furthermore, this work provides a new context for the application of XSBRL-modified binders, which have been predominantly studied in cementitious systems. Both Li et al.[15] and Li et al.[16] investigated XSBRL as a modifier for cement and soybean-flour adhesives, respectively, focusing on improving mechanical strength and adhesion. Our study differs fundamentally by using XSBRL not just as an adhesive or strength enhancer but as a dedicated toughening and energy-absorbing agent within a thermoset polymer matrix. The microstructural analysis confirms that the XSBRL phase does not simply coexist with the PHR but actively interacts with the fracture front, a key distinction from its role in cement hydration.

Finally, regarding economic feasibility, the proposed composite offers a distinct advantage over traditional synthetic surfaces. The formulation allows for a high loading of MCS – an abundant, low-cost mineral aggregate – which significantly reduces the volume fraction of the polymer binder required. Given that industrial-grade phenolic resins are generally more cost-efficient than high-performance thermoplastic polyurethanes, this reduced reliance on expensive petrochemical derivatives suggests that the XSBRL-modified composite represents not only a mechanically superior but also a commercially viable solution for large-scale court construction.

Despite the promising results, this study has limitations that present avenues for future research. First, the evaluation was conducted under laboratory conditions using standardized mechanical testers. While these devices (e.g., the portable impact tester and tribometer) provide essential objective data and ensure reproducibility, they inherently simplify the complex, active neuromuscular responses and kinematic adaptations of real athletes during gameplay. Therefore, while the measured parameters strongly correlate with injury risk reduction, future on-court trials with human subjects would provide valuable in-situ validation. Additionally, long-term durability assessments involving UV exposure, thermal cycling, and moisture ingress are necessary to predict the material's in-service lifespan. Second, the environmental impact, including the lifecycle analysis of the composite and the potential release of microplastics from wear, was not assessed. Future investigations should incorporate these aspects to provide a holistic evaluation. Finally, while this paper focused on mechanical and biomechanical properties, exploring the composite's acoustic and thermal characteristics could further enhance its suitability for indoor arenas, potentially improving user comfort and reducing noise.

4 CONCLUSION

This research successfully developed and characterized an XSBRL-modified PHR composite for basketball court applications. The key findings are:

1. The optimal XSBRL: A 12 % XSBRL amount provided the optimal combination of MPs, achieving a 90-day CS of 68 MPa and a FS of 4.5 MPa, demonstrating excellent long-term stability.

2. Superior biomechanical profile: The composite exhibited an impact absorption of 55 %, significantly outperforming traditional hardwood and polyurethane materials, alongside a performance-level rebound coefficient of 88 %.

3. Optimized surface properties: The material provides a static coefficient of friction of 0.68 and a rotational friction of 38 N·m, placing it in the ideal range to maximize athletic performance while minimizing injury risk.

4. Toughening mechanism: SEM analysis confirmed that the addition of XSBRL induced a brittle-to-ductile fracture transition, enhancing the material's toughness

and energy absorption capabilities by effectively arresting crack propagation.

These findings validate that XSBRL-modified PHR composites are a highly promising materials for constructing next-generation basketball courts that offer a superior combination of durability, safety, and athletic performance.

5 REFERENCES

[1] Y. Antoranz, E. S. de Villarreal, J. Vecino, S. L. Jiménez-Saiz, Sure Steps: Key Strategies for Protecting Basketball Players from Injuries – A Systematic Review, J. Clin. Med., 13 (**2024**) 16, 4912, doi:10.3390/jcm13164912

[2] J. Zheng, Common lower extremity injuries in sports and their recovery and preventive measures, Third Int. Conf. Biolog. Eng. Med. Sci. (ICBioMed2023), United Kingdom 2024, 582–588

[3] L. Min, N. Li, P. Bi, B. Gao, Machine learning-based prediction model for sports injury risk in biomechanics: A case study of joint injuries in basketball at a university in Xi'an, Mol. Cell. Biomech., 21 (**2024**) 4, 796, doi:10.62617/mcb796

[4] J. C. Wang, C. Li, X. Q. Zhou, Decoding the court: Insights into basketball training and performance optimization through time-motion analysis, Edu. Inform. Technol., 29 (**2024**) 18, 24459–24488, doi:10.1007/s10639-024-12783-z

[5] T. Zhao, The impact of fatigue on the jumping mechanics and injury risk of basketball players, Mol. Cell. Biomech., 22 (**2025**) 2, 1026, doi:10.62617/mcb1026

[6] N. Aksovic, S. Bubanj, B. Bjelica, M. Kocic, L. Lilic, M. Zelenovic, D. Stankovic, F. Milanovic, L. Pajovic, I. Capric, V. Milic, T. Dobrescu, C. Sufaru, Sports Injuries in Basketball Players: A Systematic Review, Life (Basel), 14 (**2024**) 7, 898, doi:10.3390/life14070898

[7] Q. H. Fan, H. Q. Duan, X. J. Xing, A review of composite materials for enhancing support, flexibility and strength in exercise, Alexandria Eng. J., 94 (**2024**) 90–103, doi:10.1016/j.aej.2024.03.048

[8] O. A. Afolabi, N. Ndou, Synergy of Hybrid Fillers for Emerging Composite and Nanocomposite Materials—A Review, Polymers, 16 (**2024**) 13, 1907, doi:10.3390/polym16131907

[9] P. Pazhamalai, V. Krishnan, M. S. M. Saleem, S. J. Kim, H. W. Seo, Investigating composite electrode materials of metal oxides for advanced energy storage applications, Nano Conver., 11 (**2024**) 1, 30, doi:10.1186/s40580-024-00437-2

[10] F. Gao, X. R. Zhang, L. Weng, Y. J. Cheng, J. H. Shi, High toughness, thermal resistance and excellent dielectric properties phenolic epoxy vinyl ester resin modified by hyperbranched polyimide, Pigm. Resin Technol., 51 (**2022**) 4, 441–448, doi:10.1108/prt-03-2021-0039

[11] J. Wu, Effect of Phenolic Resin and Nano-Calcium Carbonate Particles on the Curing Kinetic of Epoxy Composites, J. Macromol. Sci. Part B-Phys., 61 (**2022**) 6, 788-795, doi:10.1080/00222348.2022.2102370

[12] S. Cheng, P. Meng, Z. X. Huang, Y. B. Wang, Preparation and High-temperature Resistance of Phenolic Resin/Silicone Rubber Ceramifiable Composites, J. Macromol. Sci. Part B-Phys., 61 (**2022**) 12, 1473–1488, doi:10.1080/00222348.2023.2197773

[13] A. E. Kujur, S. Goswami, Effect of variation of biobased phenolic resin content in natural rubber blend on rheological, thermal and tribological properties, J. Elastom. Plast., 57 (**2025**) 3, 346–367, doi:10.1177/00952443251317115

[14] H. W. Qiao, B. R. Yang, B. T. Zheng, M. F. Chen, R. Cardinaels, P. Moldenaers, K. Lamnawar, A. Maazouz, H. G. Zhang, Janus nanoparticles as efficient interface compatibilizer in blends of polylactide and elastomers: Importance of interfacial relaxation on toughening, J. Rheol., 68 (**2024**) 5, 765–783, doi:10.1122/8.0000826

[15] H. Y. Li, H. J. Kang, W. Zhang, S. F. Zhang, J. Z. Li, Physicochemical properties of modified soybean-flour adhesives enhanced by carboxylated styrene-butadiene rubber latex, Int. J. Adhes. Adhes., 66 (**2016**), 59–64, doi:10.1016/j.ijadhadh.2015.12.008

[16] X. H. Li, R. T. Liu, S. C. Li, C. Y. Zhang, J. L. Li, B. C. Cheng, Y. K. Liu, C. Y. Ma, J. Yan, Effect of SBR and XSBRL on water demand, mechanical strength and microstructure of cement paste, Constr. Build. Mater., 332 (**2022**) 16, 127309, doi:10.1016/j.conbuildmat.2022.127309